Temperature-programmed reduction with NO as a characterization of active Cu in Cu-CHA catalysts for NH3-SCR

Temperature-programmed reduction with NO as a characterization of active Cu in Cu-CHA catalysts for NH_3-SCR

Peter S. Hammershøi[a], Chiara Negri[b], Gloria Berlier[b], Silvia Bordiga[b], Pablo Beato[c] and Ton V. W. Janssens*[a]

Abstract

Temperature programmed reduction with NO (NO-TPR) is introduced as a characterization method, by monitoring the reduction of Cu^{II} to Cu^{I} in a mixture of NH_3 and NO. Since the NO-TPR method is based on the oxidation and reduction half cycles of the NH_3-SCR reaction, quantitative information about the amount of active Cu in Cu-CHA is obtained. Furthermore, information on the stability and reactivity of reaction intermediates in the NH_3-SCR cycle is obtained as well. The reduction of the Cu is followed by monitoring the consumption of NO, after oxidation of the catalyst in O_2 or a mixture of NO and O_2 to form the Cu^{II} state. Two distinct states of the Cu are revealed. The first state, corresponding to the reduction of a Cu-oxide species, is reduced around 130 °C and is observed at low Cu content only. The second state corresponds to the reduction of a Cu-nitrate species around 200–230 °C. The low-temperature activity of Cu-chabazite catalysts with low Cu content show the same trend as the Cu-nitrate species observed in NO-TPR. The fraction of Cu-oxide in NO-TPR decreases with increasing Cu content, leading to a non-linear dependence of the NH_3-SCR activity on the Cu-content. At high Cu content, all Cu forms a stable Cu-nitrate species, and the NH_3-SCR activity becomes proportional to the Cu content. This agrees well with the known behavior of Cu-CHA catalysts, indicating that NO-TPR seems to be a viable method for the characterization of Cu-CHA materials as NH_3-SCR catalysts.

1 Introduction

The catalytic properties of Cu-CHA materials have been studied extensively during the past decade. The Cu-CHA catalysts typically have a Si/Al ratio in the range 5–20, and the excess negative charge of the zeolite is compensated by positively charged H^+ and Cu ions. These

exchanged Cu ions have the ability to change the oxidation state between Cu^{I} and Cu^{II}, dependent on the gas atmosphere and temperature.[1–8] This implies that these ions have specific redox properties that can be exploited for oxidation catalysis.

The two most studied reactions catalyzed by Cu-CHA are the direct partial oxidation of methane to methanol and the selective catalytic reduction of NO with ammonia in the presence of oxygen (NH_3-SCR).[7,9–17] The direct oxidation of methane to methanol could provide an alternative process for methanol production that circumvents the costly steam-reforming of methane to produce the mixtures of H_2, CO and CO_2, on which the current technology for large-scale methanol synthesis is based.

For NH_3-SCR, Cu-CHA materials are very efficient and robust catalysts, with both a high activity at around 200 °C, and a high hydrothermal stability up to about 700 °C.[18,19] These materials are therefore well suited for application in automotive diesel exhaust aftertreatment systems, and are already applied today in heavy-duty vehicles. The Cu-CHA catalyst makes it possible to meet the latest requirements (*e.g.* Euro 6d) for NO_x emissions from diesel engines.

In the NH_3-SCR reaction, the NO and NH_3 react to N_2 and H_2O, according to the equation $4\ NH_3 + 4\ NO + O_2 \rightarrow 4\ N_2 + 6\ H_2O$. In recent years, significant progress has been made in understanding the mechanism for this reaction.[3,4,7,20–23] The NH_3-SCR reaction cycle can actually be performed stepwise on Cu-zeolite catalysts, by alternating the oxidation and reduction steps.[1,4,20–22] In the reduction step, the Cu starts in the Cu^{II} state and is reduced to Cu^{I} in a mixture of NO and NH_3, and, dependent on the conditions, a $[Cu^{I}(NH_3)_2]^+$-complex is formed. In the oxidation part, this Cu^{I} is reoxidized to a Cu^{II} species by a reaction with an NO/O_2 mixture.

The oxidation part of the standard NH_3-SCR reaction involves the dissociation of molecular oxygen, and in the presence of NO, a Cu-nitrate is formed.[4,24,25] According to DFT calculations, molecular oxygen is expected to adsorb exclusively on a Cu^{I} species,[4,26,27] which implies that a Cu^{II} species does not contribute to the activation of O_2. The simplest scenario of oxygen dissociation on a Cu-ion is then that an oxygen molecule adsorbs on a single Cu-ion, where it dissociates. In the presence of NO, this seems a possible reaction path.[26,27]

If the O_2 molecule can interact with two Cu^{I}-ions simultaneously, to form a Cu–O_2–Cu-type of species, the dissociation of the O_2 becomes easier.[21,26–28] The activation of oxygen over such a pair of Cu-ions seems to be relevant for the NH_3-SCR reaction at low temperatures.[22] Under these reaction conditions, the Cu^{I} species is present as a linear $[Cu^{I}(NH_3)_2]^+$-complex,[4,20–22,27,29] and DFT calculations indicate that direct dissociation of an O_2 molecule on a single $[Cu^{I}(NH_3)_2]^+$-complex

does not occur.[21,22,27] The observation that the rate of oxidation of $[Cu^{I}(NH_3)_2]^+$-complexes in a CHA zeolite with O_2 shows a second order dependence on Cu-concentration further supports the conclusion that the oxidation of $[Cu^{I}(NH_3)_2]^+$-complexes in a Cu-zeolite involves pairs of $[Cu^{I}(NH_3)_2]^+$-complexes.[21,22,28] The presence of NO also seems to enhance the activation of O_2 on pairs of bare Cu^{I} ions or $[Cu^{I}(NH_3)_2]^+$-complexes.[26–28]

An obvious way to form pairs of Cu ions that interact with a single O_2 molecule is by having two Cu ions in positions close enough for a direct interaction with a single O_2 molecule. Since the Cu-ions in the ion-exchange positions in a zeolite are linked to the aluminium atoms, the ability to form Cu pairs increases with decreasing Si/Al ratio in the zeolite. This is part of the explanation why, in general, Cu-zeolites with a Si/Al ratio in the range 5–20 are preferred catalysts for the NH_3-SCR reaction.

After the initial discovery of the possible existence of the $[Cu^{I}(NH_3)_2]^+$-complex in Cu-CHA catalysts,[29] it was also realized that this complex is only weakly bound to the zeolite framework, and it therefore becomes mobile.[4,30,31] The mobility of the $[Cu^{I}(NH_3)_2]^+$-complex is another way to form the Cu pairs that can activate the O_2 molecule. The weak interaction to the zeolite enables the $[Cu^{I}(NH_3)_2]^+$-complex to move up to about 9 Å away from its Si–O–Al anchor point in the zeolite framework.[21,28] This means that the actual active sites for O_2 activation in NH_3-SCR are not present in the Cu-CHA material, but are formed dynamically under the influence of the NH_3-SCR conditions, which also allow for the formation of the $[Cu^{I}(NH_3)_2]^+$-complex. A consequence is that not all Cu present in the Cu-CHA catalyst necessarily participates in the NH_3-SCR reaction, as the limited mobility will lead to a non-zero probability that a given Cu ion does not find a second Cu-atom to form a pair.[21] This is a possible explanation for the second-order dependence of the low-temperature NH_3-SCR activity of Cu-CHA catalysts on the Cu content, as observed at low Cu contents.[23] At higher Cu contents, the fraction of unpaired Cu decreases and the activity becomes linearly dependent on the Cu content.[21] A second consequence is that the NH_3-SCR reaction necessarily follows a different mechanism at temperatures where the mobile $[Cu^{I}(NH_3)_2]^+$-complex is not stable. This change in reaction mechanism has been proposed as the reason for the decrease in SCR rate with increasing temperature, which occurs around 300 °C and agrees well with the measurement of the thermal stability of the $[Cu^{I}(NH_3)_2]^+$-complex.[7,20,22,27,32]

The dynamic formation of the active centers in a Cu-CHA catalyst implies that characterization of the Cu-CHA materials not necessarily gives information that is relevant for

the NH_3-SCR reaction. Here, we introduce temperature-programmed reduction with NO (NO-TPR) as a method for exploring the reduction and oxidation properties of Cu-CHA materials that are relevant for NH_3-SCR. The NO-TPR procedure is based on the ability to perform the NH_3-SCR reaction in alternating oxidation and reduction steps, as described above. It has been shown that the reduction in the NH_3-SCR reaction requires the presence of both NH_3 and NO.[1,4,8] By following the consumption of NO under controlled heating in an NO/NH_3 atmosphere, the reduction properties of the Cu for NH_3-SCR in the Cu-CHA catalysts are revealed. The reduction properties of Cu-CHA catalysts have been studied earlier with H_2-TPR, as a method to study the redox properties of Cu-CHA catalysts.[7,18,33–35] Even though the reduction of Cu with H_2 gives some information about the oxidation state of the Cu-CHA materials, the reduction in H_2 is not necessarily relevant in the context of the NH_3-SCR reaction. Since the reduction in a mixture of NO and NH_3 is also part of the NH_3-SCR reaction itself, the reduction as observed in NO-TPR directly reflects the reduction of the Cu species as it occurs in the NH_3-SCR reaction. Therefore, it is expected that a fraction of Cu not contributing to the NH_3-SCR activity, *e.g.* due to the limitations to form Cu-pairs as discussed above, has a different characteristic in NO-TPR, allowing for a more direct monitoring the fraction of NH_3-SCR active Cu in Cu-CHA.

In this article, we develop and explore the NO-TPR method in a study of the redox properties of Cu-CHA catalysts for NH_3-SCR. The oxidized and reduced states of the Cu-CHA catalysts are characterized by *in situ* X-ray absorption near-edge structure (XANES) spectroscopy and *in situ* Fourier-transform infrared spectroscopy (FTIR), and the importance of the sample pretreatment in NO-TPR is discussed. Then, to obtain a better insight in the relation between redox properties and NH_3-SCR activity with Cu-content, we present NO-TPR results for a series of Cu-CHA catalysts, based on the same parent material with a Si/Al ratio of 15, with different Cu contents. We show how the reduction properties of Cu-CHA change with Cu content, and relate these to the NH_3-SCR activity at 200 °C (low-temperature activity) of the Cu-CHA catalysts. We show that the ability of Cu-CHA catalysts to form a stable $[Cu^{II}(NO_3)]^+$-species in oxidation in an NO/O_2 mixture follows a similar trend with the Cu-content as the NH_3-SCR activity, suggesting that these $[Cu^{II}(NO_3)]^+$-species indicate the fraction of active Cu in Cu-CHA catalysts.

2 Experimental

To characterize the oxidation states of the Cu-CHA catalysts with the NO-TPR procedures, a set of catalysts with Si/Al ratios of 30, 15, and 5 was used, with a Cu-content of 1.7, 2.1, and 1.8 wt% Cu, respectively. These catalysts were prepared by ion-exchange of the parent materials with a 1.5 mM Cu-acetate solution, followed by calcination at 500 °C for 3 hours.

To study the relation between the reduction properties of Cu-CHA catalysts and their NH_3-SCR activity with Cu-content, a second set of six Cu-CHA catalysts with Si/Al = 15.1 and a Cu content ranging from 0.8 to 3.5 wt% was used. To avoid variations in NH_3-SCR activity not due to Cu-content, this set of catalysts was prepared by Cu-ion exchange of the same H-CHA parent material, thus excluding effects caused by variations in the zeolite itself. Portions of the H-CHA parent material were ion-exchanged with solutions of Cu-acetate with different concentrations in the range 0.5–10 mM, followed by calcination at 500 °C. Table 1 gives a more detailed overview of these catalysts. The Cu content, as measured by ICP, was corrected with the measured dry matter content of the catalyst to obtain the Cu content with respect to the amount of dry zeolite. The dry matter content of the catalysts was determined from measurement of the weight loss upon heating to 200 °C, using a Mettler Toledo HX204 moisture analyzer. The Cu/Al ratio is calculated on the basis of the Cu-content on a dry-matter basis and the known Si/Al ratio of 15.1 of the parent material, under the assumption that the Si is present as SiO_2, Al is present as AlO_2H, and Cu is present as CuO. The Cu/Al ratio is then given by:

$$\frac{N_{Cu}}{N_{Al}} = \frac{x_{Cu}\left(\frac{N_{Si}}{N_{Al}} M_{SiO_2} + M_{AlO_2H}\right)}{M_{Cu} - x_{Cu} M_{CuO}}$$

where N_{Si}, N_{Al} and N_{Cu} are the molar amounts of Si, Al, and Cu atoms, x_{Cu} is the weight fraction of Cu on a dry-zeolite basis, and M indicates the molar mass for a unit of SiO_2, AlO_2H, Cu, or CuO.

Table 1 Measured Cu content by ICP and dry matter content, Si/Al ratio and the corresponding Cu/Al ratio and Cu content on dry matter basis for the catalysts used

	Cu content ICP	Dry matter			CU content (dry matter basis)	
Catalyst	wt%	wt%	Si/Al	Cu/Al	wt%	mmol g^{-1}
A	0.717	89.7	15.1	0.123	0.799	0.126
B	1.232	90.7	15.1	0.210	1.358	0.214
C	1.629	89.4	15.1	0.284	1.822	0.287
D	1.93	91.9	15.1	0.328	2.100	0.330
E	2.625	91.5	15.1	0.453	2.869	0.451
F	3.142	90.4	15.1	0.554	3.476	0.547

In situ X-ray absorption near edge structure spectroscopy (XANES) experiments were done at the BM23 beamline of the European Synchrotron Radiation Facility (ESRF). The Cu-CHA powder was pressed in a self-supporting wafer with mass optimized for XANES measurements in transmission mode (≈100 mg, resulting in $\Delta\mu x = 0.5$ with total absorption after the edge of $\mu x = 2.5$). The wafer was mounted in a Microtomo reactor cell, equipped with an integrated heating system. The gas atmosphere was controlled by a gas manifold with four gas lines, containing He, O_2, 1% NO/He, and 1% NH_3/He connected to the reactor cell *via* mass flow controllers, allowing for adjustment of the gas atmosphere. A total flow of 100 Nml min^{-1} was used.

The XANES measurements were done using a double-crystal Si(111) monochromator for the incident energy scan. The incident (I_0) and transmitted (I_1) intensities were measured using ionization chambers placed before and after the sample cell. To calibrate the energy scale, a Cu foil reference was measured simultaneously by means of a third ionization chamber (I_2). The spectra were collected with a constant energy step ($\delta E = 0.5$ eV, 0.5 s per step). The presented spectra were normalized to unity edge jump, using the Athena software from the Demeter package.

The *in situ* FTIR spectra were recorded in transmission mode on a Perkin Elmer system 2000 infrared spectrophotometer, equipped with a MCT detector. For each scan, 128 interferograms, recorded at 2 cm^{-1} resolution, were averaged. The catalyst powders were pressed in self-supporting pellets of approximately 15 mg and placed inside a commercial FTIR reactor cell

(AABSPEC, no. 2000-Amultimode) with controlled gas atmosphere and temperature. The gas atmosphere in the cell was controlled using a gas manifold similar to that used for the XANES measurements, using He, O_2, 0.1% NO/He, and 0.1% NH_3/He. The flow used in the experiments was 50 Nml min^{-1}.

The measurements of the NH_3-SCR activity and NO-TPR measurements were done in a microreactor setup for powder samples. The reactor is mounted *via* a 4-way valve that allows for bypassing the reactor. The concentrations of NO, NO_2, N_2O, H_2O, and NH_3 are monitored with an FTIR spectrometer (Gasmet CX4000) at the reactor outlet; the composition of the feed gas is measured by bypassing the reactor.

For the activity measurements, a 5 mg sample (based on dry matter, sieve fraction 150–300 μm) of the catalysts was filled into a quartz U-tube reactor with an inner diameter of 2 mm. Before starting the measurements, the catalysts were heated at 550 °C in 10% O_2/N_2 for 1 h. Then, the feed gas was changed to 225 Nml min^{-1} NH_3-SCR feed gas, consisting of 500 ppm NO, 533 ppm NH_3, 5% water, 10% O_2, and balance nitrogen. The temperature was stepwise lowered to 500, 450, 400, 350, 300, 280, 250, 230, 220, 210, 200, 190, 180, 170, and 160 °C, and at each temperature, the system was allowed to stabilize for 20 min. To evaluate the NH_3-SCR activity, the rate constant for NH_3-SCR at 200 °C is determined from the measured conversion of NO at that temperature, under the assumption that the NH_3-SCR reaction is first order in NO. The rate constant at 200 °C (k_{200}) is then given by:

$$k_{200} = \frac{W}{F} \ln(1 - X)$$

where W is the mass of catalyst, F is the total flow, and X is the conversion of NO_x.

For the NO-TPR measurements, a catalyst powder sample of about 50 or 100 mg on a dry matter basis (150–300 μm sieve fraction) in a quartz U-tube reactor with an inner diameter of 4 mm was used. Various procedures were used for the NO-TPR measurements, which are explained in more detail in the following.

3 The NO-TPR method

The idea behind the NO-TPR experiments is to exploit the possibility of performing the NH_3-SCR reaction in separate oxidation and reduction steps to characterize the NH_3-SCR-active Cu in Cu-CHA catalysts. In the first part of the NO-TPR experiment, the Cu is brought in a Cu^{II}-state. This involves typically, but not necessarily, an exposure of the catalyst to a mixture of NO and O_2. The actual NO-TPR measurement is the reduction of this Cu^{II}-state in a mixture of NO and NH_3 during heating at a predefined rate. The changes in the NO concentration during the reduction give the NO-TPR data. The consumption of NH_3 due to reduction of the Cu^{II} is obscured by adsorption and desorption of NH_3 on the zeolite, and hence, it is difficult to obtain reliable quantitative data on the reduction from the measured NH_3 consumption. In contrast, NO interacts weakly with the zeolite, and therefore, the reduction of the Cu is clearly observed in the consumption of the NO during reduction.

To ensure a well-defined state of the catalyst in the NO-TPR, the experimental procedure consists of three parts, namely:

1. The preparation of the Cu^{II} state.

2. Equilibrating the Cu^{II} state in a mixture of NH_3 and NO at 50 °C, the start temperature for the temperature ramp.

3. Heating of the catalyst in the NO/NH_3 mixture to 370 °C, while recording the consumption of NO.

Variations in the preparation of the Cu^{II} state are possible, and this actually affects the final consumption of NO during the reduction. For the NO-TPR data presented here, the exposure to the NO/O_2 mixture is preceded by a reduction step in NO/NH_3 at 200 °C, which corresponds to the situation in the NH_3-SCR reaction, or by an oxidation in O_2 at 500 °C.

We have chosen to start the reduction at 50 °C, which is the lowest practicable temperature in our equipment. Since the NH_3-SCR reaction, and therefore also the reduction in the NO/NH_3 mixture, is already very effective at 200 °C, the reduction must be started at a significantly lower temperature, in order to detect the NO consumption during reduction. To achieve a well-defined and reproducible state of the catalyst starting the reduction by heating, the Cu^{II}-state is equilibrated at 50 °C until the adsorption of NH_3 on the zeolite is completed, and the measured concentrations of NO and NH_3 correspond to the inlet concentrations.

Fig. 1 gives an overview of the concentrations of NO, NO_2, N_2O, NH_3 and O_2 during the entire procedure for NO-TPR, using 55 mg of catalyst E. The shaded areas indicate the steps in the pretreatment of the catalyst, *i.e.* heating to 500 °C, reduction in NO/NH_3 at 200, oxidation in NO/O_2 at 50 °C to prepare the Cu^{II} state, exposure to NO/NH_3 at 50 °C to equilibrate, and finally

the NO-TPR step in NO/NH_3 during heating to 370 °C. Immediately before each pretreatment step, the reactor was bypassed to mix the feed gas to the appropriate concentration, and to measure the composition of the feed gas at each stage. The analysis of the reduction of the Cu-CHA catalysts is based on the consumption of NO during heating to 370 °C (blue curve in red shaded area).

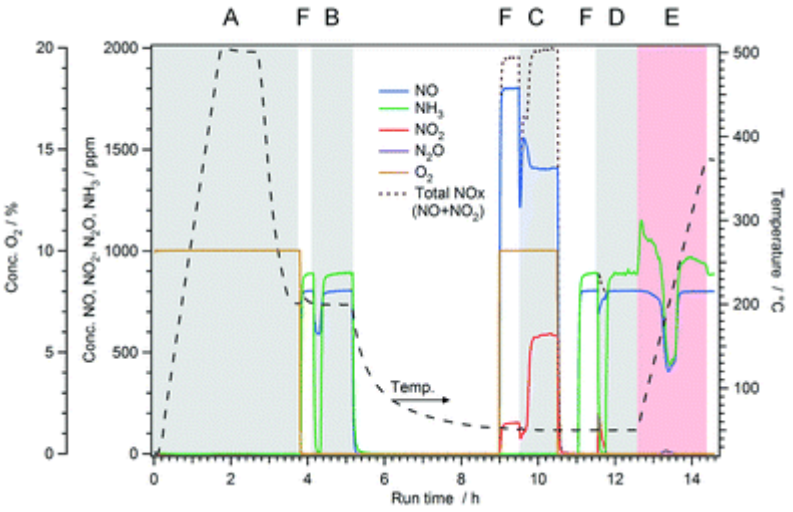

Fig. 1 Concentrations of NO, NH_3, NO_2, N_2O, O_2 and temperature during the entire procedure for an NO-TPR measurement. Top letters indicate the different phases of the experiment: A: Heating in O_2 to 500 °C; B: Reduction in NO/NH_3 at 200 °C; C: Exposure to NO/O_2 at 50 °C; D: Exposure to NO/NH_3 at 50 °C; E: TPR in NO/NH_3; F: Reactor bypassed for feed measurement.

Before turning our attention to the analysis of NO-TPR data, we first discuss a few observations during the different reduction and oxidation before starting the temperature-programmed reduction step. When the NO/NH_3-mixture is admitted to the reactor at 200 °C in the reduction step, some NO is consumed, indicating that that the Cu is in an oxidized state after heating to 500 °C in O_2. Simultaneously, a much larger amount of NH_3 is consumed, because additional NH_3 is consumed for the formation of the linear $[Cu^{I}(NH_3)_2]^+$-complex and adsorption of NH_3 on the Brønsted sites in the zeolite at 200 °C.

After the reduction at 200 °C, in which the linear $[Cu^{I}(NH_3)_2]^+$-complex is formed,[4] the catalysts are oxidized at 50 °C in a mixture of 2000 ppm NO and 10% O_2, which yields a Cu^{II}–(N,O) phase. Fig. 1 shows that about 60 ppm NO_2 is formed in this mixture, due to the spontaneous oxidation of NO that occurs in the gas phase. Exposing the reduced catalyst to this NO/O_2 mixture at 50 °C leads to a further oxidation of NO, to yield approximately 160 ppm of NO_2.

This increase in NO_2 concentration corresponds to the oxidation of NO to NO_2 in the confined spaces of the zeolite.[36] For this article, it is important to note that some NO_2 has been present during this oxidation step, but we do not address this formation of NO_2 further.

Finally, before the NO-TPR run can be started, the oxidized Cu^{II}–(N,O) phase must be exposed to the mixture of NO and NH_3 at 50 °C. The ammonia adsorption that occurs under these conditions leads to the delayed breakthrough of the ammonia. Furthermore, a small amount of NO is consumed initially, together with a larger release of NO_2. This shows that at least a part of the Cu^{II}–(N,O) phase reacts with NO and possibly also with NH_3 at 50 °C, indicating that already at this temperature, some Cu^{II}–(N,O) species reacts with NH_3 and NO. The release of NO_2, however, is not compatible with a complete NH_3-SCR reaction, which only produces N_2 and H_2O. It may indicate the reaction between a $[Cu^{II}(NO_3)]^+$ species and NO, which can release NO_2 into the gas phase; this reaction would not change the oxidation state of the Cu.[4,24]

The changes of the Cu-CHA during the NO-TPR procedure have been verified by the Cu K-edge XANES spectra and FTIR, which are shown in Fig. 2. In the Cu-K edge XANES spectrum, the reduction of Cu-CHA at 200 °C in the NO/NH_3 mixture followed by cooling to 50 °C in He results leads to an intense pre-edge peak at 8983 eV(Fig. 2, red). This peak is due to the 1s → 4p transitions in Cu^I compounds with a low coordination number. This indicates the formation of the $[Cu^I(NH_3)_2]^+$-complex,[2,4,7,8,20,21,29,30,32] confirming that the Cu is present as Cu^I at this stage. The formation of the $[Cu^I(NH_3)_2]^+$-complex is corroborated by FTIR, showing the infrared band at 1620 cm^{-1} related to NH_3 coordinated to Cu ions. The band at 1446 cm^{-1} and shoulder at 1416 cm^{-1} are due to NH_4^+,[29] formed by adsorption of NH_3 on the Brønsted sites of the zeolite during the reduction at 200 °C.

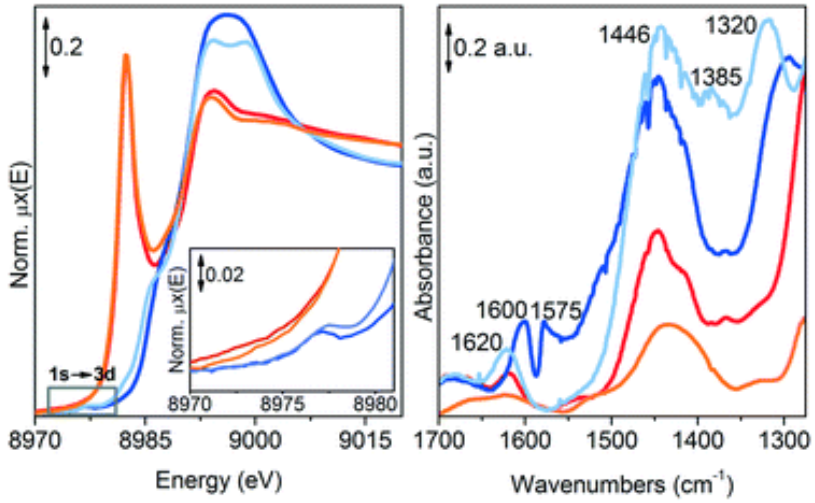

Fig. 2 Left panel: Cu K-edge XANES spectra of catalyst B at different stages in the NO-TPR procedure: after reduction in NO/NH_3 at 200 °C and subsequent cooling in He to 50 °C (red); after exposure of the reduced Cu to NO/O_2 at 50 °C (blue); after re-exposure to NO/NH_3 at 50 °C (light blue), and after heating to 300 °C in NO/NH_3. The inset shows a magnification of the 1s → 3d Laporte-forbidden transition (grey box), which indicates the presence of a Cu^{II}-state. Right panel: Same steps followed by FTIR spectroscopy on catalyst D.

After subsequent exposure of the $[Cu^{I}(NH_3)_2]^+$-complex to the NO/O_2 mixture at 50 °C, the characteristic XANES Cu-K pre-edge peak disappears, and a typical spectrum for a Cu^{II} state is obtained (Fig. 2, blue). The appearance of the weak Laporte-forbidden 1s →3d transition (see inset left panel in Fig. 2) is evidence for a Cu^{II} state. The shape of the XANES spectrum is reminiscent of the spectra obtained upon oxidation in NO/O_2 at 200 °C, which were shown to be due to $[Cu^{II}(NO_3)]^+$-species.[4] The formation of a nitrate species is clearly observed in FTIR by the bands at 1600 and 1575 cm^{-1}, which is characteristic for a bidentate $[Cu^{II}(NO_3)]^+$-species.[4,25,37] The intense band at 1300 cm^{-1} and the parallel increase at 1446 cm^{-1} indicates the presence of some monodentate nitrate species as well.[25,38] This means that the exposure of $[Cu^{I}(NH_3)_2]^+$ to a NO/O_2 mixture at 50 °C leads to oxidation of the Cu and formation of a Cu^{II}–(N,O)-species, probably $[Cu^{II}(NO_3)]^+$.

Re-exposure of this Cu^{II}–(N,O)-species to the NO/NH_3 mixture at 50 °C does not substantially change the oxidation state of the Cu. In the XANES spectrum, the weak 1s →3d transition is still present, and only a small change is observed in the Cu-K pre-edge region (Fig. 2, light blue). The shape of the white line changes and resembles that in the spectra of the $Cu^{II}(NH_3)_4^{2+}$-complex.[4,32] Indicating a change in the first coordination of Cu ions, due to coordination of the Cu by NH_3. The coordination of the $[Cu^{II}(NO_3)]^+$-species by ammonia is also observed in FTIR. The

band at 1620 cm^{-1}, indicative of coordination of Cu by NH_3, reappears. The bands around 1300 and 1440 cm^{-1} persist, indicating that monodentate nitrate species still are present. Furthermore, a band at 1385 cm^{-1}, characteristic for ammonium nitrate,[39] appears, while the bands at 1575 and 1600 cm^{-1} for $[Cu^{II}(NO_3)]^+$ disappear. This indicates that the nitrate species becomes more "ammonium-nitrate-like" upon coordination of the Cu with NH_3. In conclusion, re-exposing the $[Cu^{II}(NO_3)]^+$ species to the NO/NH_3 mixture at 50 deg C results in coordination of the Cu by NH_3 to form $Cu^{II}(NH_3)_x(NO_3)_2^+$-complexes ($x < 4$), without a change in the oxidation state of the Cu.

Finally, heating in NO/NH_3 restores the original $[Cu^{I}(NH_3)_2]^+$ complex (Fig. 2, orange), indicating that the Cu-CHA indeed is reduced the NO-TPR step.

4 Results

The results presented above show that the reduction of Cu^{II} in NO/NH_3 takes place between 50 and 300 °C. Fig. 3 shows the NO-TPR profiles of Cu-CHA catalysts with a Si/Al of 30, 15, and 5 and Cu-contents of 1.7, 2.1, and 1.8 wt%, respectively. For each catalyst, two NO-TPR profiles are shown, obtained by exposing a reduced or oxidized form of the Cu-CHA catalyst to the NO/O_2 mixture at 50 °C. In general, we see that there are two reduction features: a feature around 130 °C, and one around 230 °C; for the catalyst with a low Si/Al ratio, these features appear at approximately 20 °C higher temperature. The two distinct regions where NO consumption takes place indicate that there are at least two different forms of oxidized Cu that are reduced in the mixture of NO and NH_3 for a wide range of Si/Al ratios in the Cu-CHA catalysts; we designate the Cu-species associated with the peak around 130 °C and 230 °C as Cu-a and Cu-b, respectively.

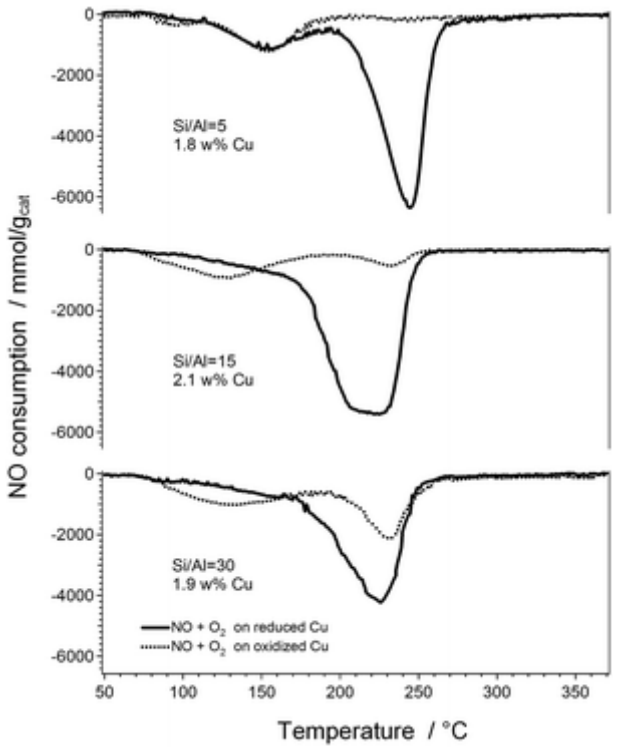

Fig. 3 NO-TPR profiles for Cu-CHA catalysts with Si/Al ratios of 30, 15, and 5, and Cu content of 1.7, 2.1 and 1.8 wt%, respectively. The different reduction profiles indicate that the formation of the Cu^{II}–(N,O)-phase at 50 °C is sensitive to the state of the catalyst, implying that the pretreatment of the catalyst is an important factor.

It is clear that the total NO consumption strongly depends on the oxidation state of the Cu catalyst under the exposure to the NO/O_2 mixture to form the Cu^{II}–(N,O)-phase. The general trend is that more NO is consumed when the NO/O_2 reacts with a reduced Cu-CHA catalyst. This emphasizes that the pretreatment of the catalyst is important for the final result of the NO-TPR measurement.

In order to measure the amount of Cu participating in the NH_3-SCR reaction, we have adopted a pretreatment procedure that mimics the NH_3-SCR reaction. In the NH_3-SCR reaction, the O_2 is activated on a Cu^{I}-species,[4,21,27] and therefore we have chosen a procedure in which the catalysts are first reduced in a mixture of 800 ppm NO and 900 ppm NH_3 at 200 °C, followed by exposure to the NO/O_2 mixture at 50 °C; this is the procedure shown in Fig. 1. Fig. 4 shows a series of NO-TPR data for the series of Cu-CHA catalysts A–F with different Cu content, as specified in Table 1. The NO-TPR step was done by heating to 370 °C at a rate of 3 °C min^{-1} in a mixture of 800 ppm NO and 900 ppm NH_3 with 200 Nml min^{-1}.

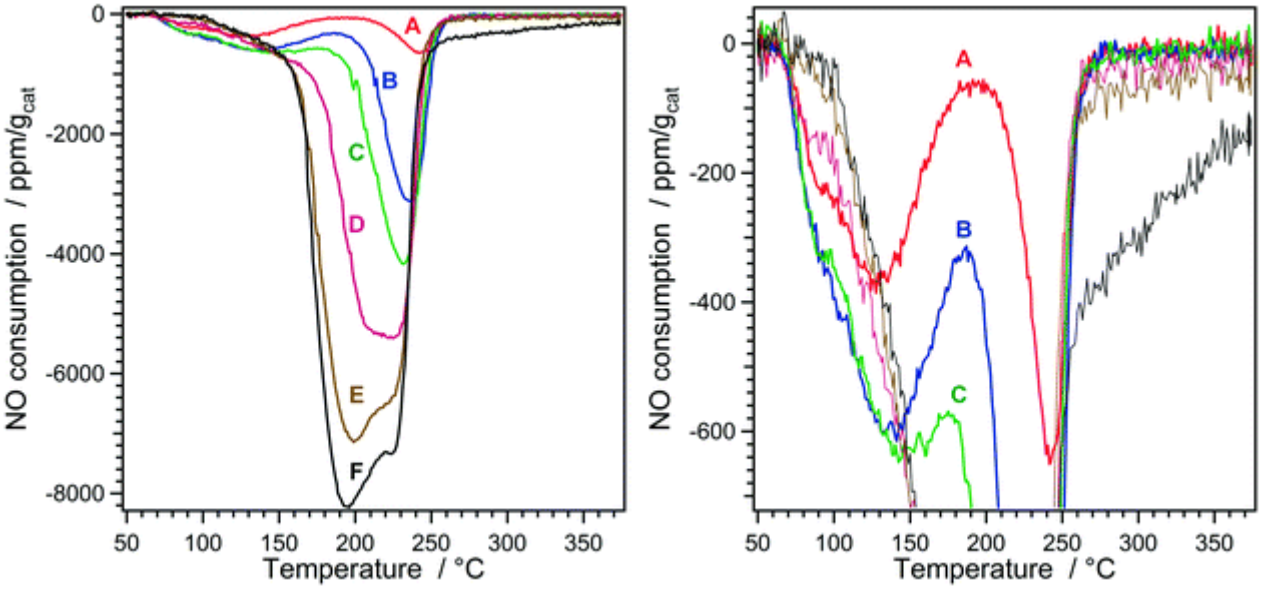

Fig. 4 Consumption of NO during reduction in 800 ppm NO/900 ppm NH_3/N_2 of Cu-CHA catalysts with different Cu content. Letters refer to the catalysts as listed in Table 1. The pretreatment consisted of reduction in NO/NH_3 at 200 °C and exposure to NO/O_2 at 50 °C. Reduction gas mixture: 800 ppm/NO/900 ppm NH_3/N_2. Flow: 200 Nml min^{-1}. Heating rate: 3 °C min^{-1}. Right panel: Magnification of the left panel, highlighting the changes in the reduction that take place around 130 °C.

For the catalysts with a low Cu-content, the two distinct temperature ranges for NO consumption, with peaks at around 130 °C and 230 °C, similar to those shown in Fig. 3 for Cu-a and Cu-b. At higher Cu content, the Cu-a-peak is not observed, and the Cu-b-peak at 230 °C widens towards the low temperature side, with the maximum NO consumption changing to just below 200 °C. The disappearance of Cu-a with increasing Cu content is highlighted in the right panel of Fig. 4, clearly showing the change in the shape of the TPR profile with increasing Cu content. The total area under the curves increases with Cu content, which is in line with the expectation that more NO is consumed when more Cu is present.

In the following, we show that Cu-a is a Cu^{II}-species that does not contain nitrogen, and that Cu-b is a $[Cu^{II}(NO_3)]^+$-species, which has already been identified spectroscopically in Fig. 2. This assignment is made on the basis of additional NO-TPR measurements, in which the procedure for the formation of the Cu^{II}-species has been varied, and a further analysis of the NO-TPR data presented in Fig. 4.

Fig. 5 presents NO-TPR curves for catalysts B and D, which were measured with and without exposure to the NO/O_2 mixture at 50 °C after oxidation of the Cu at 500 °C in O_2. The NO-TPR curves for catalyst B, with the Cu^{II}–(N,O) species formed from reduced Cu are included as a reference (see also Fig. 4). If the exposure to NO/O_2 is omitted in that case, then there is no significant NO consumption. This is expected, since the catalyst has not been oxidized after the initial reduction at 200 °C, leaving the catalyst in the reduced state when performing the NO-TPR measurement.

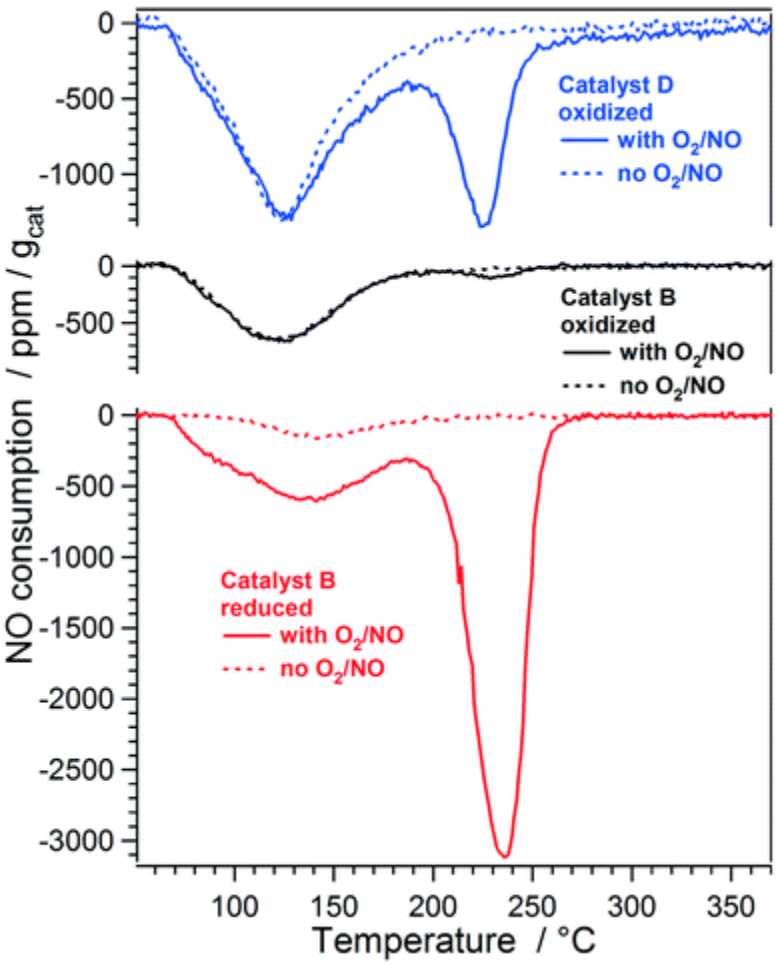

Fig. 5 NO-TPR profiles with and without exposure to the NO/O_2 mixture at 50 °C for oxidized Cu-CHA (catalysts B (black) and D (blue)) and for reduced Cu-CHA (catalyst B (red)). All graphs are drawn to the same scale.

If the oxidized Cu-CHA catalyst is exposed to the NO/O_2 mixture at 50 °C, the NO-TPR shows both the Cu-a peak at 130 °C and the Cu-b peak at 230 °C. At low Cu content (catalyst B), the Cu-b remains small (catalyst B, 1.35 wt% Cu), but it becomes clearly visible for a catalyst with a higher

Cu content (catalyst D, 2.1 wt% Cu). If the exposure to the NO/O_2 mixture at 50 °C is omitted, the peak Cu-b peak disappears, while the Cu-a-peak is not affected. These results lead to several important conclusions:

• The Cu-b species is a nitrogen-containing Cu^{II}-species. This is based on the observation that the NO-TPR peak around 230 °C is only observed after oxidation of the catalyst in the NO/O_2 mixture, while it is not present after oxidation in O_2 only.

• The formation of the Cu-b species is enhanced when the NO/O_2 mixture reacts with the reduced Cu^{I}-species, probably $[Cu^{I}(NH_3)_2]^+$, which is formed by reduction in NO/NH_3 at 200 °C. Exposure of Cu^{II} to the NO/O_2 mixture at 50 °C results in a significantly smaller NO-TPR peak around 230 °C, indicating a smaller amount of the Cu-b species.

• The Cu-a species is a Cu^{II}-species that does not contain nitrogen, since it is enhanced after oxidation in O_2 at 500 °C, and can also be formed without exposure to the NO/O_2 mixture. This means that the Cu-a species does not react with NO alone. The most obvious candidates for the Cu-a species are Cu^{II}-oxide or hydroxide.

We have now established that the Cu-b species corresponds to a nitrogen-containing Cu^{II}-species. Aquantitative analysis of the NO-TPR peak at 230 °C indicates that the nitrogen-containing Cu^{II}-species is a $[Cu^{II}(NO_3)]^+$, as follows. By integration of the NO-TPR data shown in Fig. 4, the total consumption of NO in the reduction is determined, and compared with the Cu content in the catalysts. From this, the number of NO molecules consumed per Cu atom is determined. Table 2 summarizes these results for the catalysts A–F. We see that the number of consumed NO molecules per Cu atom equals 3 for the catalysts with a higher Cu content (D, E, and F). For the catalysts with a lower Cu-content, the NO/Cu ratio becomes lower. It is noted that precisely the catalysts where the Cu-a species is found also show a NO/Cu ratio lower than 3. A graph of these data is given in Fig. 6, showing that the catalysts D, E, and F fall on the dashed line, which indicates the stoichiometric NO/Cu ratio of 3.

Table 2 Total NO consumption (mmol g^{-1}) and NO/Cu ratio in NO-TPR of Cu-CHA catalysts, after exposure of reduced Cu-CHA catalysts to a mixture of 800 ppm NO and 900 ppm NH_3, and corresponding conversion of NO and rate constants for NH_3-SCR

Catalyst	Cu cont. (ICP)	Total NO cons. TPR	NO/Cu ratio	NO cons. at 120 °C (Cu-a)	NO cons. at 230 °C (Cu-b)	Total Cu(II)[a]	NO_x conv. (200 °C)	SCR rate constant (200 °C)
		mmol g^{-1}		mmol g^{-1}	mmol g^{-1}	mmol g^{-1}		mol g_{cat}^{-1} s^{-1} bar^{-1}
A	0.126	0.129	1.02	0.07	0.059	0.090	0.039	0.92
B	0.214	0.446	2.08	0.13	0.316	0.235	0.104	2.78
C	0.287	0.602	2.10	0.11	0.492	0.274	0.194	4.91
D	0.330	0.990	3.00	0.03	0.960	0.350	0.230	5.98
E	0.451	1.359	3.01	0	1.359	0.453	0.294	8.40
F	0.547	1.630	2.98	0	1.630	0.543	0.316	9.33

[a] The total amount of Cu^{II} is calculated as the sum of the NO consumption at 130 °C and 1/3 of the consumption at 230 °C.

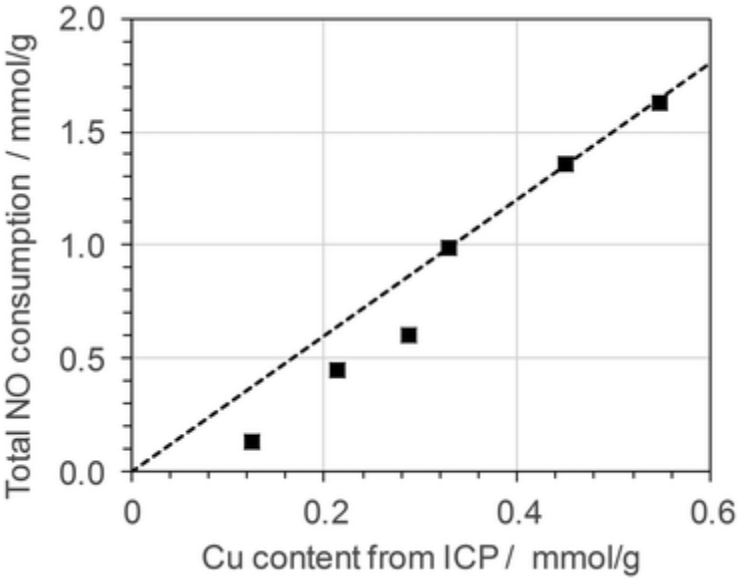

Fig. 6 Total consumption of NO in NO-TPR as a function of the Cu content in Cu-CHA catalysts, after exposure of the reduced state of the Cu-CHA catalysts to a mixture of 800 ppm NO and 900 ppm NH_3. The dashed line corresponds to the stoichiometric ratio NO/Cu of 3.

The stoichiometric NO/Cu ratio of 3 points to the reduction of $[Cu^{II}(NO_3)]^+$. In an earlier publication, we presented a reaction cycle for NH_3-SCR, in which a $[Cu^{II}(NO_3)]^+$ species reacts with NO to form a $[Cu^{II}(NO_2)]^+$ species and an NO_2 (g) molecule, followed by further reduction with NH_3 and NO to Cu^I.[4] According to that reaction cycle, the net reaction for the reduction of the $[Cu^{II}(NO_3)]^+$ can be written as:

$$[Cu^{II}(NO_3)]^+ + 3\ NO\ (g) + 4\ NH_3\ (g) \rightarrow 4\ N_2\ (g) + 6\ H_2O\ (g) + [Cu^{I}]^+$$

Eqn (3) shows that the reduction of a $[Cu^{II}(NO_3)]^+$ species in an NO/NH_3 mixture requires 3 NO molecules per Cu atom. Therefore, the observed consumption of 3 NO molecules per Cu atom indicates that, for the catalysts with a Cu content above 2 wt% (catalysts D, E, F), all Cu is present as $[Cu^{II}(NO_3)]^+$ species in the NO-TPR measurement. The NO-TPR profile for these catalysts show only the presence of the Cu-b species, which therefore can be assigned to the $[Cu^{II}(NO_3)]^+$ species. In addition to the spectroscopic identification of the $[Cu^{II}(NO_3)]^+$ species given in Fig. 2, electron paramagnetic resonance (EPR) measurements also reveal the formation of $[Cu^{II}(NO_3)]^+$ in reactions of the $[Cu^{I}(NH_3)_2]^+$-complex with NO/O_2 mixtures.[4,8,24,25,37,40] Furthermore, the NO consumption in a $(NH_3 + NO)$-TPSR measurement on a Cu-CHA catalyst with adsorbed nitrates, which is essentially the same as the NO-TPR measurements presented here, shows a consumption of NO that is quite similar to our curves, especially when the nitrate phase is formed at 120 °C,[24] which is closest to the conditions used here.

We note that eqn (3) does not contain the $[Cu^{I}(NH_3)_2]^+$-complex as the Cu^{I} phase explicitly. The presence of the $[Cu^{I}(NH_3)_2]^+$-complex, however, can be easily accounted for by balancing the NH_3 (g) or by the presence of additional NH_3-ligands on the $[Cu^{II}(NO_3)]^+$-complex, without affecting the stoichiometric factors for NO and Cu.

The catalysts with a lower Cu content (catalysts A, B, and C) show the presence of the Cu-a species in the NO-TPR profiles (see Fig. 4 and 5), which we assign to a Cu^{II}-oxide or hydroxide species. This means that for Cu-CHA catalysts with a lower Cu content, not all Cu atoms form a stable $[Cu^{II}(NO_3)]^+$ species and the stoichiometric ratio NO/Cu becomes lower than 3. Starting from a $[Cu^{II}O]^+$, which can be regarded as one half of a dimeric $[Cu^{II}–O_2–Cu^{II}]^{2+}$ species, the reduction to Cu^{I} in an NO/NH_3 mixture can be written as follows:

$$[Cu^{II}O]^+ + 2\ NO\ (g) + 2\ NH_3\ (g) \rightarrow 2\ N_2\ (g) + 3\ H_2O\ (g) + [Cu^{I}]^+$$

In a similar manner, the reduction of a $[Cu^{II}OH]^+$-species, to Cu^{I} follows the equation:[4,22,41]

$$2[Cu^{II}OH]^+ + 2\ NO\ (g) + 2\ NH_3\ (g) \rightarrow 2\ N_2\ (g) + 4\ H_2O\ (g) + 2\ [Cu^{I}]^+$$

Eqn (4) and (5) show that the stoichiometric NO/Cu ratio for the reduction of the Cu-a species is expected to be between 1 and 2, dependent on the type of Cu-oxide species in the catalyst. In any case, this lower than 3, in full agreement with the experimental result (Table 2). Assuming a stoichiometric factor of 1 for the Cu-a species, the total amount of Cu^{II}, as determined from the NO-TPR data, matches the Cu content obtained with ICP for all catalysts, except for catalyst A (see Table 2). For catalyst A, the total amount of Cu^{II} determined from the NO-TPR data is lower, indicating that either not all Cu has been oxidized, or that there could be another Cu^{II} phase that is not reduced in the NO/NH_3-mixture at 200 °C.

To relate the NO-TPR results to the low-temperature NH_3-SCR activity of the catalysts A–F, we have measured the NO_x conversion in the temperature range 160–550 °C, which is shown in the left panel of Fig. 7. The right panel in Fig. 7 displays the first order rate constant for the NH_3-SCR reaction at 200 °C, calculated according to eqn (2); the values for the NO_x conversion and rate constants are also included in Table 2. The development of the rate constants with the total Cu content, as determined by ICP, is shown by the red squares in Fig. 7, right panel. These data follow the familiar pattern for Cu-CHA catalysts, with a disproportionally low activity for catalysts with low Cu content.[23] This could mean that there exists a critical Cu content for NH_3-SCR activity of Cu-CHA catalysts. There are also indications that the NH_3-SCR activity at low Cu content actually is proportional to the square of the Cu content, which would also explain this pattern.[21,23] The latter explanation has led to the conclusion that the NH_3-SCR reaction actually requires pairs of Cu ions, which are formed through diffusion of mobile $[Cu^{I}(NH_3)_2]^+$-complexes.

The NO-TPR results presented above show that the Cu-CHA catalysts contain both Cu-a and Cu-b species, while catalysts with a high Cu content only have Cu-b. This suggests that the disproportionally low activity of the Cu-CHA catalysts with low Cu content is related to the presence of the Cu-a species, and that only Cu-b, which is able form a stable $[Cu^{II}(NO_3)]^+$, contributes to the low-temperature NH_3-SCR activity. To verify this hypothesis, we also compare the rate constants with the amount of Cu-b, which is determined as 1/3 of the amount of NO consumed around 230 °C (see Fig. 4 and Table 2). The blue dots in the right panel in Fig. 7 show this comparison, and we see, that in the catalysts with low Cu content, the activity becomes proportional to the amount of Cu-b, supporting the hypothesis that only Cu-b contributes to the low-temperature NH_3-SCR activity in these catalysts.

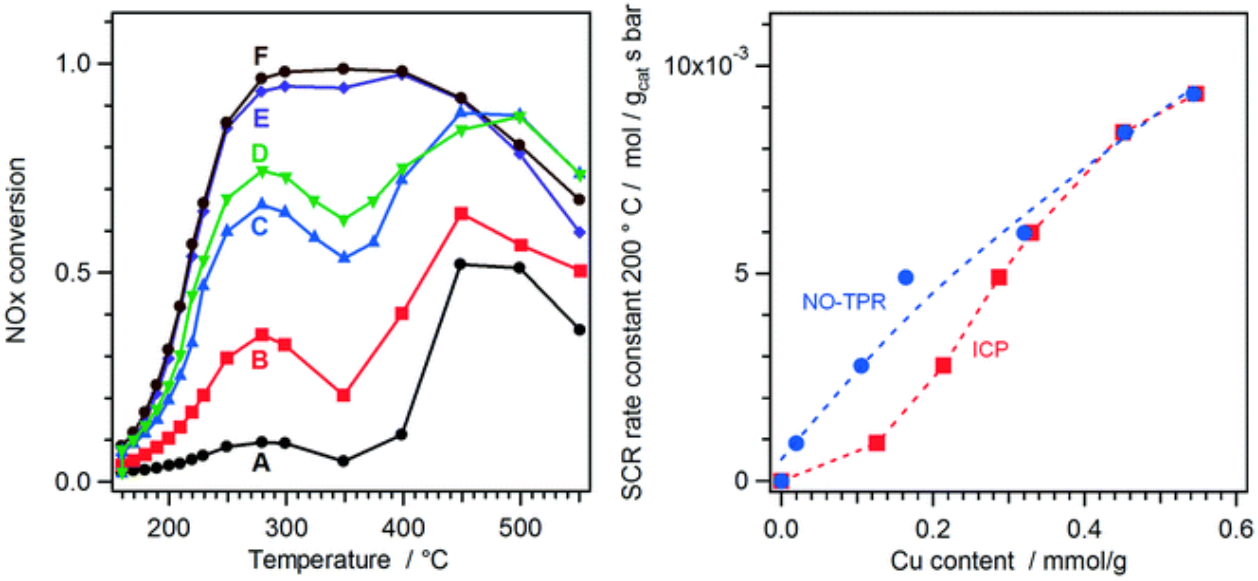

Fig. 7 Left: Measured NO_x conversion for catalysts A–F, (feed gas: 500 ppm NO, 533 ppm NH_3, 5% H_2O, 10% O_2, balance N_2; flow: 225 Nml min^{-1}, 5 mg catalyst). Right: NH_3-SCR activity expressed as 1st order rate constants at 200 °C as a function of the total Cu content (ICP, red) and the amount of Cu-b ($[Cu^{II}(NO_3)]^+$) from NO-TPR (blue).

5 Discussion

The NO-TPR results clearly indicate the presence of two types of Cu in Cu-CHA catalysts, that are distinguished by the reaction product of the oxidation of Cu^I ($[Cu^I(NH_3)_2]^+$) with a mixture of NO and O_2. One type of Cu, Cu-b, forms a stable $[Cu^{II}(NO_3)]^+$ species, and the other type, Cu-a, forms a Cu-oxide or Cu–OH species. If the Cu content is sufficiently high, all Cu in a Cu-CHA catalyst is Cu-b, while in catalysts with a lower Cu content, some Cu-a is present as well. The low-temperature NH_3-SCR activity is shows the same trend as the $[Cu^{II}(NO_3)]^+$ (Cu-b) phase in NO-TPR, resulting in a linear correlation with the measured activity in catalysts with low Cu content. Since the formation of $[Cu^{II}(NO_3)]^+$ is enhanced on a reduced Cu-CHA (Fig. 5), it is important that the amount of $[Cu^{II}(NO_3)]^+$ is formed starting from reduced Cu, to reflect the oxidation step in the NH_3-SCR reaction correctly. The observation that the $[Cu^{II}(NO_3)]^+$ species is reduced in a NO/NH_3 mixture in the range 150–250 °C implies that it is reactive under typical conditions for NH_3-SCR, and therefore, it cannot be a spectator species in an NH_3-SCR reaction.

The reason for the correlation between Cu-b and the NH_3-SCR activity is that the formation of $[Cu^{II}(NO_3)]^+$ from Cu^I or $[Cu^I(NH_3)_2]^+$ is part of the NH_3-SCR reaction cycle.[4] In both the formation of $[Cu^{II}(NO_3)]^+$ and the NH_3-SCR reaction, the dissociation of O_2 on the Cu^I or $[Cu^I(NH_3)_2]^+$ species is an essential step. Since O_2 does not interact with Cu^{II} in a Cu-CHA catalyst,[4,26,27,37] activation of O_2 requires a Cu^I species. The observation that the formation of $[Cu^{II}(NO_3)]^+$ is enhanced when the

NO/O_2 mixture after reduction of the Cu-CHA catalyst in NO/NH_3 (Fig. 5) provides direct experimental evidence of this, as the formation of a $[Cu^{II}(NO_3)]^+$-species must involve the dissociation of the O_2 molecule. The requirement of a Cu^I for O_2 dissociation also implies that the rate of NO-oxidation to NO_2 over Cu-CHA does not directly reflect the oxidation properties of Cu-CHA relevant for NH_3-SCR, as the Cu-CHA will contain much less Cu^I under the conditions for NO-oxidation with O_2, which therefore is much slower.[6,42]

The clear reduction observed in NO-TPR after exposure of a reduced Cu to a mixture of NO and O_2 at 50 °C (Fig. 5) indicates that the oxidation of Cu^I already takes place at that temperature, which is further corroborated by Cu K-edge XAS (see Fig. 2). The reduction associated with the Cu-b species, starts between 150 and 200 °C, which is close to the light-off temperature for NH_3-SCR on Cu-CHA catalysts. This would indicate that the oxidation of Cu^I is easier, which is not consistent with earlier conclusions that the dissociation of oxygen is the rate-limiting step for the NH_3-SCR reaction.[4,21,22,26] It seems that the unavoidable presence of NO_2 in the NO/O_2 mixture is relevant here. Oxidation by NO_2 is more efficient, and therefore, the oxidation of Cu^I in the NO/O_2 mixture probably is due to NO_2. A lower temperature for oxidation of Cu^I with NO_2, compared to the reduction in NO/NH_3, indicates that NO_2 indeed can enhance the rate of the NH_3-SCR reaction to give the fast-SCR reaction. Consequently, the oxidation in NO/O_2 as used in the NO-TPR procedure described in this article corresponds to the oxidation for a fast-SCR reaction, $4\,NH_3 + 2\,NO + 2\,NO_2 \rightarrow 4\,N_2 + 6\,H_2O$, rather than the standard NH_3-SCR reaction. This would also indicate that the reduction in NO/NH_3 becomes rate determining in fast-SCR. Following the reaction mechanism for NH_3-SCR as proposed earlier,[4] the reduction in standard-NH_3-SCR and fast-SCR follow identical pathways, and therefore, the reduction profiles in NO-TPR as presented here also reflect the reduction as it occurs in the standard NH_3-SCR reaction.

The data in Table 2 show that the total amount of Cu^{II} determined from NO-TPR, assuming a stoichiometric factor NO/Cu-a of 1, matches the amount found from ICP, indicating that all Cu is oxidized in the NO-TPR measurements. Recently, it has been shown that in oxidation of the Cu^I species in O_2, some of the Cu^I phase persists, while oxidation in NO_2 leads to a complete oxidation.[21] This agrees well with the conclusion that all Cu has been oxidized by NO_2 present in the NO/O_2 mixture (see Fig. 1). This means that at least a part of the Cu^{II} phase in the NO-TPR experiments is formed by a direct reaction between Cu^I and NO_2. Then, the oxidic Cu-a species in NO-TPR is the result of a decomposition of a Cu–(N,O) species, rather than the product of

oxidation by O_2, and consequently, some of the Cu in the Cu-CHA catalysts does not form stable $[Cu^{II}(NO_3)]^+$ or other Cu^{II}–(N,O) species. For such an oxidic Cu-species formed by decomposition of Cu^{II}–(N,O) species, it can be expected that these do not react further in the NO/O_2 mixture, in line with our conclusion for the Cu-a species in the NO-TPR measurements. An exception is catalyst A, in which there can be a larger contribution of a $Cu^{II}O$ phase, according to eqn (4), or some reduced Cu may still be present during the NO-TPR measurement, since there is a difference between the amount of Cu^{II} in NO-TPR and the total amount of Cu found by ICP.

Measurements with electron paramagnetic resonance (EPR) also indicate that, at least at low Cu content, a part of the visible Cu species remains unaffected upon exposure to NO and O_2, also indicating that not all Cu is able to form a stable $[Cu^{II}(NO_3)]^+$.[40] The fact that such a Cu species is observed in EPR also means that it is a Cu^{II} species, since Cu^{I} species are EPR silent. This matches the assignment of the Cu-a species well: it must be a Cu^{II} species, because NO-TPR shows that it can be reduced in the NO/NH_3 mixture, but it is not affected by the exposure to the NO/O_2 mixture. Furthermore, the Cu-a species is only observed for the Cu-CHA catalysts with a low Cu content. Therefore, the Cu-a species observed in NO-TPR may very well be the same Cu species as the one that does not form a $[Cu^{II}(NO_3)]^+$ species in EPR.

An interesting aspect is that increasing the Cu content results the disappearance of Cu-a, which follows directly from the changes in the NO-TPR profiles around 130 °C, as highlighted in Fig. 4. This suggests that a higher fraction of the Cu becomes active with increasing Cu content, and that at only at sufficiently high Cu contents (>2 wt%) all Cu contributes to the NH_3-SCR activity. This corresponds to the known linear dependence of the NH_3-SCR activity with Cu content in this range. For Cu-CHA catalysts containing less Cu, the fraction of Cu-b increases with the Cu-content, and the dependence of the NH_3-SCR activity becomes non-linear, with an increasing turnover frequency per Cu atom, in agreement with the known behavior of Cu-CHA catalysts.[21,23]

The disappearance of the Cu-a species seems to be accompanied by the development of a second $[Cu^{II}(NO_3)]^+$ species, with a reduction temperature just below 200 °C; this becomes particularly clear for catalysts E and F (see Fig. 4). A quantification of this second $[Cu^{II}(NO_3)]^+$ species, however, is difficult due to the unknown shape of the corresponding NO-TPR peak and the significant overlap with those for the $[Cu^{II}(NO_3)]^+$ species around 230 °C and the oxidic Cu-a species. The possibility of forming two different types of $[Cu^{II}(NO_3)]^+$ species at 50 °C

has been presented in a recent study of the formation of Cu^{II}–(N,O) species using FTIR.[25] One type is influenced by the presence of the Brønsted H^+ sites in the zeolite, and is characterized by an IR band at 1625 cm^{-1}, in the absence of NH_3. This type is more prominent in catalysts with a low Cu content. The other type, with IR bands at 1610 and 1575 cm^{-1}, is less affected by the presence of the Brønsted sites, and develops at higher Cu loading.[25] Following this reasoning, the NO-TPR peak around 230 °C is then due to $[Cu^{II}(NO_3)]^+$ close to a Brønsted site in the zeolite, and the NO-TPR peak just below 200 °C is due to $[Cu^{II}(NO_3)]^+$ not interacting with a Brønsted site. This would imply that Brønsted sites have a stabilizing effect on $[Cu^{II}(NO_3)]^+$, which leads to a higher reduction temperature. The broadening of the NO-TPR peak as shown in Fig. 4 is then due to a development of a $[Cu^{II}(NO_3)]^+$ phase that does not interact with Brønsted sites. This interpretation would also explain the somewhat higher reduction temperature for a Cu-CHA catalyst with low Si/Al ratio, shown in Fig. 3, as such a catalyst has a larger amount of Brønsted sites, shifting the reduction temperature of $[Cu^{II}(NO_3)]^+$ to higher temperatures.

6 Conclusions

We have introduced temperature programmed reduction with NO (NO-TPR) as a method to obtain direct and quantitative information about the reduction of the Cu^{II} species in Cu-CHA catalysts. In the NO-TPR procedure, a mixture of NO and NH_3 is used to reduce the Cu^{II} species, and the consumption of NO is measured as a function of the temperature. Since this procedure reflects the reduction part of the NH_3-SCR reaction in Cu-CHA catalysts, the observed reduction profiles are a direct reflection of the relevant reduction properties of Cu for the NH_3-SCR reaction.

The reduction of Cu-CHA catalyst in NO/NH_3 mixtures generally takes place in the temperature range 100–250 °C. Often two peaks are observed, representing the reduction of a Cu-oxide or Cu-hydroxide around 130 °C, and the reduction of one or more Cu-nitrate ($[Cu^{II}(NO_3)]^+$) around 200–230 °C. At low Si/Al ratio, the reduction shifts to about 20 °C higher temperature. The results of the NO-TPR measurement further depend on the way the Cu^{II} phase is prepared, as a consequence of a different reactivity of the NO/O_2 mixture with reduced and oxidized Cu. The general trend is that more Cu-nitrate is formed in a reaction with reduced Cu.

To determine the amount of Cu participating in the NH_3-SCR reaction at low temperatures, good results were obtained by first preparing a Cu^{I} phase in a mixture of 800 ppm NO and 900 ppm NH_3 followed by oxidation at 50 °C in a mixture of 2000 ppm NO in 10% O_2/N_2. The NO-TPR

results for series of Cu-CHA catalysts for NH_3-SCR, with different Cu content, ranging from 0.8 to 3.5 wt%, on the same parent material (Si/Al = 15), show a distinction between catalysts with a low and high Cu content.

At high Cu content, the NO consumption in the NO-TPR takes place between 150 and 250 °C, in a broader reduction peak with a maximum consumption at around 200–230 °C. In these cases, the total NO consumption corresponds to exactly 3 times the Cu content in the catalysts, which confirms that all Cu in the catalyst is present as a $[Cu^{II}(NO_3)]^+$ species, as identified by spectroscopic techniques. This also implies that the $[Cu^{II}(NO_3)]^+$ species is active under typical SCR conditions.

The low-temperature activity of the Cu-CHA catalysts is related to the amount of stable $[Cu^{II}(NO_3)]^+$ that is observed in the NO-TPR measurement. For Cu-CHA with a low Cu content, this means that a certain fraction of the Cu does not contribute to the low-temperature NH_3-SCR activity. Increasing the Cu content leads to a gradual increase in the fraction of active Cu, leading to a non-linear dependence of the low-temperature NH_3-SCR activity on the Cu content. At sufficiently high Cu content, all Cu participates in the NH_3-SCR reaction, which is reflected in the amount of stable $[Cu^{II}(NO_3)]^+$ as determined by NO-TPR. This leads to a linear dependence of the NH_3-SCR activity on the Cu content, in agreement with the known trend of the low-temperature NH_3-SCR activity with Cu content in Cu-CHA catalysts.

Notes and references

1. S. Kieger, G. Delahay, B. Coq and B. Neveu, *J. Catal.*, 1999, **183**, 267–280
2. J. S. McEwen, T. Anggara, W. F. Schneider, V. F. Kispersky, J. T. Miller, W. N. Delgass and F. H. Ribeiro, *Catal. Today*, 2012, **184**, 129–144
3. C. Paolucci, A. A. Verma, S. A. Bates, V. F. Kispersky, J. T. Miller, R. Gounder, W. N. Delgass, F. H. Ribeiro and W. F. Schneider, *Angew. Chem., Int. Ed.*, 2014, **53**, 11828–11833
4. T. V. W. Janssens, H. Falsig, L. F. Lundegaard, P. N. R. Vennestrøm, S. B. Rasmussen, P. G. Moses, F. Giordanino, E. Borfecchia, K. A. Lomachenko, C. Lamberti, S. Bordiga, A. Godiksen, S. Mossin and P. Beato, *ACS Catal.*, 2015, **5**, 2832–2845
5. T. Günter, H. W. P. Carvalho, D. E. Doronkin, T. Sheppard, P. Glatzel, A. J. Atkins, J. Rudolph, C. R. Jacob, M. Casapu and J. D. Grunwaldt, *Chem. Commun.*, 2015, **51**, 9227–9230
6. T. Günter, D. E. Doronkin, A. Boubnov, H. W. P. P. Carvalho, M. Casapu and J. D. Grunwaldt, *Top. Catal.*, 2016, **59**, 866–874
7. E. Borfecchia, P. Beato, S. Svelle, U. Olsbye, C. Lamberti and S. Bordiga, *Chem. Soc. Rev.*, 2018, **47**, 8097–8133
8. A. Marberger, A. W. Petrov, P. Steiger, M. Elsener, O. Kröcher, M. Nachtegaal and D. Ferri, *Nat. Catal.*, 2018, **1**, 221–227
9. F. Gao, J. H. Kwak, J. Szanyi and C. H. F. Peden, *Top. Catal.*, 2013, **56**, 1441–1459
10. A. M. Beale, F. Gao, I. Lezcano-Gonzalez, C. H. F. Peden and J. Szanyi, *Chem. Soc. Rev.*, 2015, **44**, 7371–7405
11. E. Borfecchia, K. A. Lomachenko, F. Giordanino, H. Falsig, P. Beato, A. V. Soldatov, S. Bordiga and C. Lamberti, *Chem. Sci.*, 2015, **6**, 548–563
12. C. Paolucci, J. D. Iorio, F. Ribeiro, R. Gounder and W. Schneider, in *Catalysis Science of NOx Selective Catalytic Reduction With Ammonia Over Cu-SSZ-13 and Cu-SAPO-34*, ed. C. Song, Academic Press, 2016, vol. 59 of Advances in Catalysis, pp. 1–107
13. M. H. Mahyuddin, A. Staykov, Y. Shiota, M. Miyanishi and K. Yoshizawa, *ACS Catal.*, 2017, **7**, 3741–3751
14. A. Martini, E. Borfecchia, K. A. Lomachenko, I. Pankin, C. Negri, G. Berlier, P. Beato, H. Falsig, S. Bordiga and C. Lamberti, *Chem. Sci.*, 2017, **8**, 6836–6851
15. F. Gao and C. H. F. Peden, *Catalysts*, 2018, **8**, 140
16. A. A. Guda, S. A. Guda, K. A. Lomachenko, M. A. Soldatov, I. A. Pankin, A. V. Soldatov, L. Braglia, A. L. Bugaev, A. Martini, M. Signorile, E. Groppo, A. Piovano, E. Borfecchia and C. Lamberti, *Catal. Today*, 2018 DOI: 10.1016/j.cattod.2018.10.071
17. A. Martini, E. Alladio and E. Borfecchia, *Top. Catal.*, 2018, **61**, 1396–1407
18. J. H. Kwak, D. Tran, S. D. Burton, J. Szanyi, J. H. Lee and C. H. F. Peden, *J. Catal.*, 2012, **287**, 203–209
19. J. Song, Y. Wang, E. D. Walter, N. M. Washton, D. Mei, L. Kovarik, M. H. Engelhard, S. Prodinger, Y. Wang, C. H. F. Peden and F. Gao, *ACS Catal.*, 2017, **7**, 8214–8227
20. C. Paolucci, A. A. Parekh, I. Khurana, J. R. Di Iorio, H. Li, J. D. A. Caballero, A. J. Shih, T. Anggara, W. N. Delgass, J. T. Miller, F. H. Ribeiro, R. Gounder and W. F. Schneider, *J. Am. Chem. Soc.*, 2016, **138**, 6028–6048
21. C. Paolucci, I. Khurana, A. A. Parekh, S. Li, A. J. Shih, H. Li, J. R. Di Iorio, J. D. Albarracin-Caballero, A. Yezerets, J. T. Miller, W. N. Delgass, F. H. Ribeiro, W. F. Schneider and R. Gounder, *Science*, 2017, **357**, 898–903

22. F. Gao, D. Mei, Y. Wang, J. J. Szanyi and C. H. F. Peden, *J. Am. Chem. Soc.*, 2017, **139**, 4935–4942
23. F. Gao, E. D. Walter, M. Kollar, Y. Wang, J. Szanyi and C. H. F. Peden, *J. Catal.*, 2014, **319**, 1–14
24. M. Colombo, I. Nova and E. Tronconi, *Catal. Today*, 2012, **197**, 243–255
25. C. Negri, P. S. Hammershøi, T. V. W. Janssens, P. Beato, G. Berlier and S. Bordiga, *Chem. – Eur. J.*, 2018, **24**, 12044–12053
26. H. Falsig, P. N. R. Vennestrøm, P. G. Moses and T. V. W. Janssens, *Top. Catal.*, 2016, **59**, 861–865
27. L. Chen, H. Falsig, T. V. W. Janssens and H. Grönbeck, *J. Catal.*, 2018, **358**, 179–186
28. L. Chen, H. Falsig, T. V. W. Janssens, J. Jansson, M. Skoglundh and H. Grönbeck, *Catal. Sci. Technol.*, 2018, **8**, 2131–2136
29. F. Giordanino, E. Borfecchia, K. A. Lomachenko, A. Lazzarini, G. Agostini, E. Gallo, A. V. Soldatov, P. Beato, S. Bordiga and C. Lamberti, *J. Phys. Chem. Lett.*, 2014, **5**, 1552–1559
30. S. Shwan, M. Skoglundh, L. F. Lundegaard, R. R. Tiruvalam, T. V. W. Janssens, A. Carlsson and P. N. R. Vennestrøm, *ACS Catal.*, 2015, **5**, 16–19
31. A. Y. Stakheev, D. A. Bokarev, A. I. Mytareva, T. V. W. Janssens and P. N. R. Vennestrøm, *Top. Catal.*, 2017, **60**, 255–259
32. K. A. Lomachenko, E. Borfecchia, C. Negri, G. Berlier, C. Lamberti, P. Beato, H. Falsig and S. Bordiga, *J. Am. Chem. Soc.*, 2016, **138**, 12025–12028
33. J. H. Kwak, H. Zhu, J. H. Lee, C. H. F. Peden and J. Szanyi, *Chem. Commun.*, 2012, **48**, 4758–4760
34. F. Gao, E. D. Walter, E. M. Karp, J. Luo, R. G. Tonkyn, J. H. Kwak, J. Szanyi and C. H. F. Peden, *J. Catal.*, 2013, **300**, 20–29 .
35. F. Gao, N. M. Washton, Y. Wang, M. Kollár, J. Szanyi and C. H. Peden, *J. Catal.*, 2015, **331**, 25–38
36. J. A. Loiland and R. F. Lobo, *J. Catal.*, 2014, **311**, 412–423
37. C. Tyrsted, E. Borfecchia, G. Berlier, K. A. Lomachenko, C. Lamberti, S. Bordiga, P. N. R. Vennestrøm, T. V. W. Janssens, H. Falsig, P. Beato and A. Puig-Molina, *Catal. Sci. Technol.*, 2016, **6**, 8314–8324
38. B. O. Field and C. J. Hardy, *J. Chem. Soc.*, 1964, 4428–4434
39. I. Nova, C. Ciardelli, E. Tronconi, D. Chatterjee and B. Bandl-Konrad, *Catal. Today*, 2006, **114**, 3–12.
40. S. Mossin, A. Godiksen, O. L. Isaksen, P. N. R. Vennestrøm and S. B. Rasmussen, *ChemCatChem*, 2017, 3–8
41. D. E. Doronkin, M. Casapu, T. Günter, O. Müller, R. Frahm and J.-D. Grunwaldt, *J. Phys. Chem. C*, 2014, **118**, 10204–10212
42. M. P. Ruggeri, I. Nova and E. Tronconi, *Top. Catal.*, 2013, **56**, 109–113